Pergamon

Journal of Structural Geology, Vol. 17, No. 8, pp. 1077 to 1093, 1995

0191-8141/95 $9.50 + 0.00

0191-8141(95)00005-4

Vorticity analysis and recognition of ductile extension in the Sanbagawa belt, SW Japan

SIMON WALLIS

Department of Geology and Mineralogy, Faculty of Science, Kyoto University, Kyoto 606-01, Japan

(*Received* 15 *January* 1993; *accepted in revised form* 28 *December* 1994)

Abstract—Metamorphic belts in the internal parts of mountain belts have invariably undergone regional penetrative deformation. Such deformation may form as the result of bulk simple shear between two essentially rigid plates or, alternatively, as a result of ductile thickening or thinning. Studies of the degree of non-coaxiality during deformation (vorticity analyses) can help distinguish between the resulting kinematic histories. Possible indicators of the degree of non-coaxiality include: (i) the rotation of porphyroclasts with different aspect ratios; (ii) the distribution of sets of material lines with different stretch histories; (iii) geometries of crystallographic fabrics; and (iv) the orientation of oblique grain shape fabrics. Application of such methods in the Sanbagawa metamorphic belt, SW Japan suggests that the dominant regional tectonic fabric, associated with orogen-parallel shearing, formed as a result of ductile extension. Quantitative analyses suggest the associated thinning was of the order of 50%. The major departure from bulk simple shear can also be related to the formation of conjugate shears with opposed senses of shear on various scales. The significant amount of thinning that took place during ductile deformation of the Sanbagawa belt shows that this tectonic phase is related to exhumation processes and not to burial during subduction. Both the thinning and its associated stretching direction (roughly orogen-parallel) may be related to oblique convergence with a gradient in the strike-slip component along the length of the orogen.

INTRODUCTION

The internal parts of mountain belts are commonly occupied by metamorphic belts that characteristically have undergone penetrative ductile deformation. There are several possible tectonic interpretations of such regional ductile fabrics. In some instances the deformation may have formed during subduction processes between two essentially rigid plates. The associated deformation should then approximate to progressive simple shear. Alternatively deformation may be related to large-scale ductile thickening or thinning of the crust. In these cases bulk deformation may approximate more closely to pure shear than simple shear. The possibility that extension and thinning may be important processes during the formation of mountain belts has attracted particular attention recently (e.g. Molnar & Tapponier 1978, Platt 1986, Royden & Burchfiel 1987, England & Houseman 1988). One of the key issues in searching for a tectonic interpretation of deformational fabrics in metamorphic belts is the extent to which deformation caused changes in thickness of the tectonic pile.

The question of whether a metamorphic sequence has been thickened or thinned as a result of high-strain deformation can, to some extent, be tackled by using syn-deformational metamorphic minerals to determine *P–T* paths. Such techniques have been successful in revealing the importance of ductile thinning in, for instance, the Eastern Alps (Selverstone 1985, 1988) and Corsica (Jolivet *et al.* 1990). There are, however, a number of potential problems with this approach: e.g. non-diagnostic mineral assemblages; growth under non-equilibrium conditions; lack of retrograde metamorphic reactions. This paper focuses on the problem of using structural data to carry out kinematic reconstructions in one particular region of penetrative ductile formation.

The Sanbagawa metamorphic belt of SW Japan has undergone regional penetrative ductile deformation characterized by a stretching lineation approximately parallel to the trend of the belt (Toriumi 1982, Faure 1985). Faure (1983, 1985) suggested that this deformation was close to simple shear and directly reflects the former plate movement. In contrast, Wallis *et al.* (1992a) emphasize the widespread, albeit incomplete, association of retrograde metamorphism with this deformation and suggested it could be related to ductile extension. These two tectonic interpretations can be distinguished by the predicted kinematic types, i.e. whether deformation caused thinning or not. The principal aim of this paper is to use the Sanbagawa belt as an example of how vorticity analysis can be applied as a structural tool for testing such hypotheses.

VORTICITY AND MEASURES OF NON-COAXIALITY

Introduction

Finite deformation can be decomposed into three independent components: finite strain (deviatoric stretch), volume change and rotation. There are many techniques available for estimating finite strain in metamorphic tectonites (see Ramsay & Huber 1983 for a review). In low-grade rocks, pressure solution and volume change can be important processes (Durney 1972,

Wright & Platt 1982, Bell & Cuff 1989). However, in higher grade rocks that have dominantly undergone deformation by processes of intracrystalline plasticity, solution transfer is commonly assumed to have played a lesser role (Kerrich *et al.* 1977, Rutter 1983) and deformation is likely to be essentially equal volume. There are numerous possible methods of estimating volume change using both structural (e.g. Passchier 1988b, Wright & Platt 1982) and chemical techniques (e.g. Gratier 1983, O'Hara 1990). In contrast to finite strain and volume change, methods for determining the rotational component of finite deformation have been relatively little studied. All three components need to be estimated to carry out a kinematic reconstruction of a deformed region.

Deformation may also be analyzed at any instant. Instantaneous deformation, or flow, can be decomposed into components of stretching rate (which includes rate of volume change) and vorticity (instantaneous rotation rate). The relationship between the contributions of vorticity and stretching rate to the flow is referred to as the degree of non-coaxiality. Studies of the degree of non-coaxiality are commonly referred to as vorticity analyses and have received relatively little attention in the geological literature. Vorticity analyses can be combined with studies of strain to estimate the rotational component of deformation.

Before looking at particular techniques of vorticity analysis, I will briefly review the continuum mechanics background and ways in which the degree of non-coaxiality has been defined.

Definitions of vorticity

General flow of a continuous medium can be expressed by the second-order tensor quantity, L_{ij} (the velocity gradients tensor), which has components of spatial gradients in velocity (v_i):

$$L_{ij} = \nabla v_i. \tag{1}$$

L_{ij} can be split into components representing instantaneous stretching rate, D_{ij}, (the rate of deformation tensor) and instantaneous rotation, W_{ij} (the vorticity tensor). If L_{ij}^{T} is the transpose of L_{ij} then D_{ij} and W_{ij} can be expressed as follows,

$$D_{ij} = \tfrac{1}{2}(L_{ij} + L_{ij}^{\mathrm{T}}) \tag{2}$$

$$W_{ij} = \tfrac{1}{2}(L_{ij} - L_{ij}^{\mathrm{T}}) \tag{3}$$

(e.g. Malvern 1969 p. 147). W_{ij} is a skew symmetric tensor representing an angular velocity vector with components:

$$\frac{1}{2}\left(\frac{\partial v_i}{\partial x_j} - \frac{\partial v_j}{\partial x_i}\right)$$

(Truesdell 1954 p. 58, Malvern 1969 p 56).

Vorticity is likewise a measure of the instantaneous rotation rate of slow but is defined slightly differently. For a given two-dimensional velocity field the vorticity, **w**, can be defined by:

$$\begin{aligned}\mathbf{w} &= \mathrm{curl} v_i \\ &= \nabla \times v_i \\ &= \left(\frac{\partial v_i}{\partial x_j} - \frac{\partial v_j}{\partial x_i}\right).\end{aligned} \tag{4}$$

By comparison with equation (3) it can be seen that the components of the angular velocity vector represented by W_{ij} are exactly half those of the vorticity vector **w**. The vorticity vector **w** can be thought of as twice the instantaneous rigid body rotation of a small element of the continuum (Truesdell 1954 p. 64).

The magnitude and orientation of **w** can be affected by the choice of reference frame. Vorticity measured with respect to a reference frame that is at a fixed angle to the instantaneous stretching axes is referred to by some authors as 'internal vorticity' (Means *et al.* 1980, Lister & Williams 1983). In many geological situations, however, it is more convenient to attach the reference frame to shear zone boundaries or to geographical coordinates which may not remain at a fixed angle to the instantaneous stretching axes of deformation. Vorticity which includes an extra angular velocity of the stretching axes with respect to an external reference frame may be referred to as external vorticity (Means *et al.* 1980, Lister & Williams 1983).

Vorticity may be zero, in which case the flow is coaxial (e.g. pure shearing). If the magnitude of **w** is non-zero then flow is non-coaxial. Positive and negative values of vorticity differ in the associated sense of rotation rate.

Degree of non-coaxiality

The flow type that results from a given magnitude of **w**, the vorticity vector, depends on the amount of simultaneously operating stretching, which is represented by D_{ij}. The relationship between the vortical and stretching components of flow is referred to as the degree of non-coaxiality, which can be expressed in terms of a vorticity number. There is a difficulty, however, in trying to express the relationship between the second-order stretching rates tensor, D_{ij} and the vorticity vector, **w**, with a meaningful scalar quantity.

The most general approach to this problem is given by Truesdell (1954 p. 107) who defines a kinematic vorticity number, W_k, as:

$$W_k = \frac{w}{\sqrt{2(s_1^2 + s_2^2 + s_3^2)}}, \tag{5}$$

where w is the magnitude of the vorticity vector and s_i are the magnitudes of the principal stretching rates of D_{ij}. A simplified vorticity number, W_n, can also be defined as

$$W_n = \frac{w}{2s} \tag{6}$$

where s is the average of the principal stretching rates s_1 and s_2 (McKenzie 1979, Bobyarchick 1986, Passchier 1988a,b). For plane-strain equal-area deformation $W_n = W_k$.

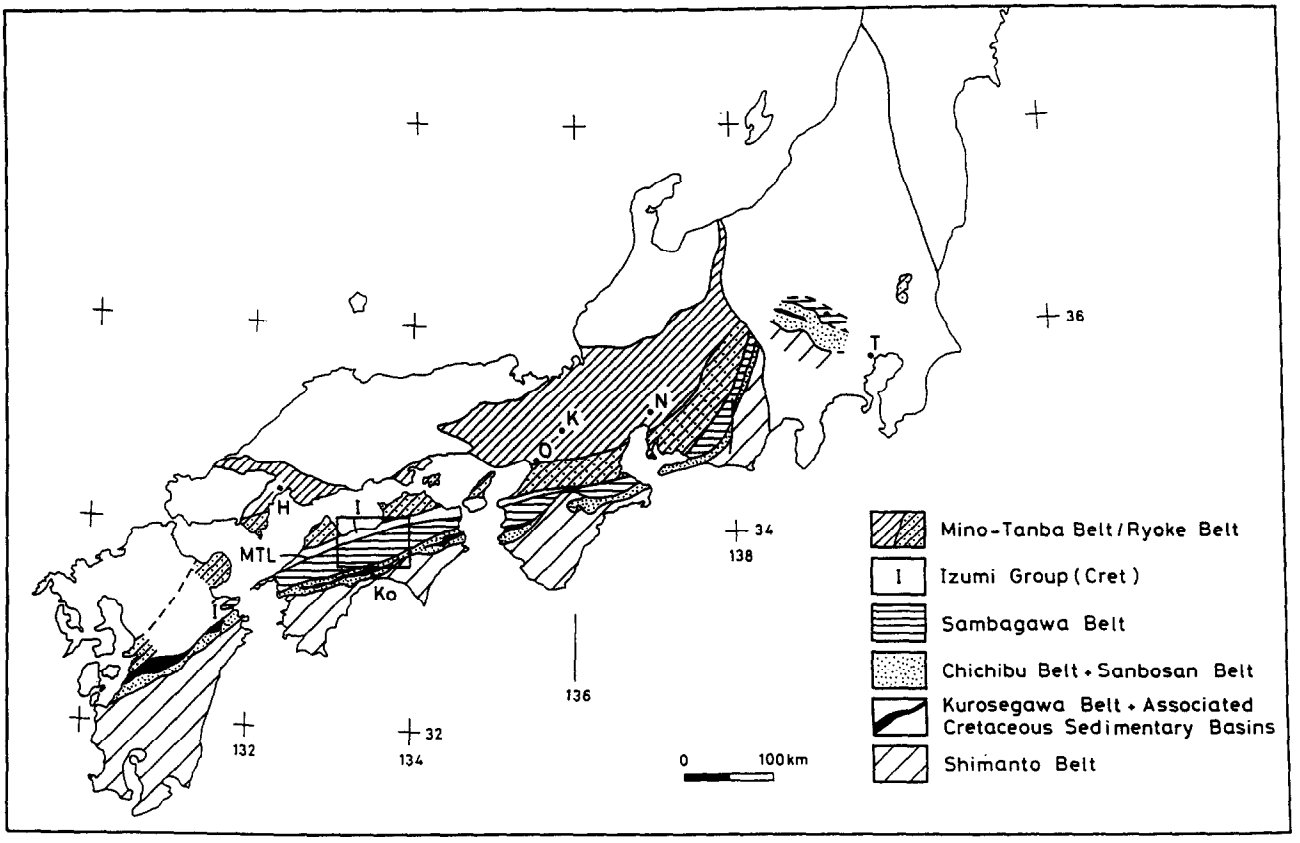

Fig. 1. Main tectonic units of SW Japan (after Wallis *et al.* 1992b). The Sanbagawa metamorphic belt is shown by horizontal stripes. MTL = Median Tectonic Line, T = Tokyo, N = Nagoya, K = Kyoto, O = Osaka, H = Hiroshima, Ko = Kochi. The location of Fig. 2 is shown by a box.

Other measures of the degree of non-coaxiality are also possible (e.g. Elliott 1972, Ghosh & Ramberg 1976, Ghosh 1987). In particular, the measure of non-coaxiality proposed by Ghosh & Ramberg (1976) has been used by a number of different workers in geological studies. Ghosh & Ramberg (1976) decompose plane-strain constant-area flow into factors of instantaneous pure and simple shearing. The simple shearing factor is associated with a shear strain rate of $\dot{\gamma}$ and the pure shearing component is associated with a stretching rate of $\dot{\varepsilon}_x$ parallel to the shear plane of the simple shearing. The quantity $S_r = \dot{\varepsilon}_x/\dot{\gamma}$ can then be used as a measure of the degree of non-coaxiality (e.g. Bobyarchick 1986, Vissers 1989, Tikoff & Fossen 1993). This is related to W_n by the equation

$$S_r = \frac{\sqrt{(1 - W_n^2)}}{2W_n} \tag{7}$$

(Passchier 1987, Vissers 1989).

The above measures of the degree of non-coaxiality are defined only for an instant of deformation. To describe finite deformation, Passchier (1988b) introduced the mean vorticity number, W_m. Finite deformation can then be decomposed into three quantities: volume change, finite (deviatoric) strain and W_m. If flow is steady state, i.e. the values of L_{ij} are constant, then $W_n = W_m$.

The vortical and stretching components of flow as well as the counterparts for finite deformation, rotation and strain, are essentially independent. The principle axes of these tensor quantities need not therefore coincide with each other. In many geological examples, however, the vorticity vector is approximately parallel to the Y axis of finite strain. This suggests that in many cases deformation can be effectively analyzed in the X–Z plane of finite deformation. Deviations from plane strain can be taken into account by including an appropriate amount of stretch along the vorticity vector. In the following I refer to the relationship between a variety of structures and the 'flow plane'. For general two-dimensional flow this is the plane with zero angular velocity with respect to the instantaneous stretching axes which is itself extending. During steady-state deformation the maximum finite elongation direction will rotate towards this plane. In the case of simple shearing the flow plane corresponds to the shear plane.

I have used a variety of techniques to assess the degree of non-coaxiality during deformation in a number of samples from the Sanbagawa belt, SW Japan. Before discussing the practical details of the vorticity analysis, the geology of this region will be introduced.

REGIONAL GEOLOGY OF THE SANBAGAWA BELT

The Sanbagawa (or Sambagawa) belt is a regionally coherent high P–T metamorphic belt that stretches for several 100 km through SW Japan (e.g. Banno & Sakai 1989, Wallis & Banno 1990, Takasu *et al.* 1994) (Fig. 1).

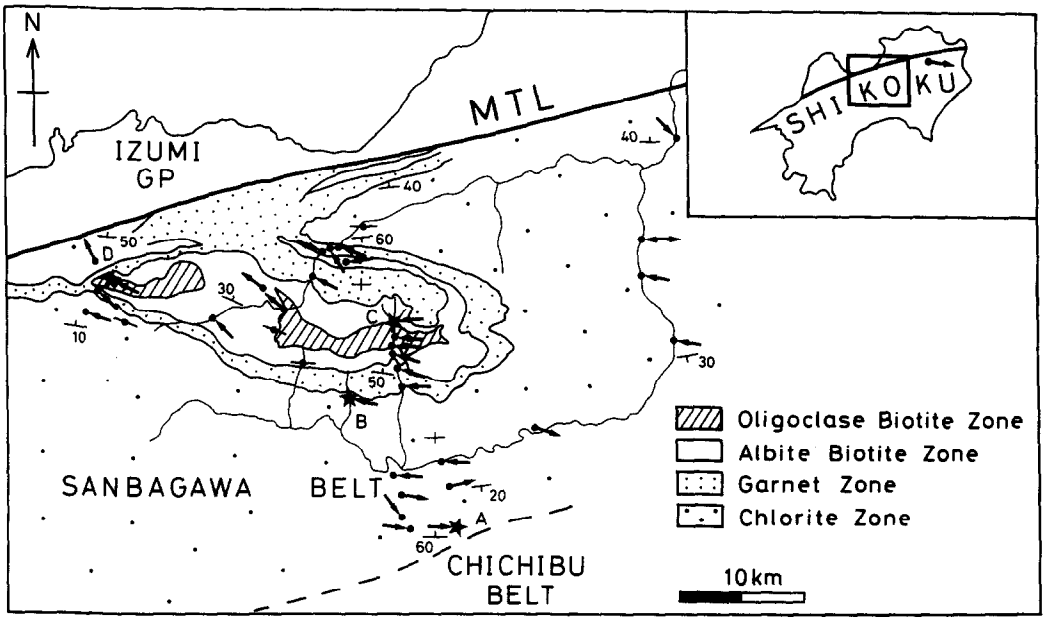

Fig. 2. Metamorphic zonal map of central Shikoku after Banno (1964) and Higashino (1990). In general the foliation dips north (Wallis *et al.* 1992a) although there is some local variation due to later folding as shown on the map. The orientation of the stretching lineation is shown by lines; the sense of shear, where known is shown by an arrowhead. Details of the sense of shear determinations are given in Wallis *et al.* (1992a). The locations of the samples used in the vorticity analyses are shown by stars and labelled A, B, C and D.

The metamorphism can be divided into four zones according to the appearance of index minerals in metapelite (Banno 1964, Higashino 1990). In increasing order of grade these are: the chlorite zone, the garnet zone, the albite–biotite zone, and the oligoclase–biotite zone. This sequence represents both an increase in peak temperature and pressure (Banno & Sakai 1989, Wallis *et al.* 1992a, Enami *et al.* 1994) and the estimated *P–T* conditions for the formation of the oligoclase–biotite zone are 10 kbar 610°C. The highest grade rocks are exposed mainly in the central part of Shikoku island and samples from this area form the focus for this study (Fig. 2).

The main phase of ductile deformation in the region can be described in terms of high-strain orogen-parallel shear associated with the development of a prominent stretching lineation (Toriumi 1982, Faure 1985, Shimizu 1988, Wallis *et al.* 1992a). The dominant deformation mechanism in the higher grade region is crystalline plasticity, and I therefore assume deformation to be essentially equal volume. Wallis (1992a) uses deformed vein arrays to show that volume change was negligible in one particular part of the region. Studies of finite strain in central and eastern Shikoku suggest that deformation on a large scale was close to plane strain (Faure 1985). This is supported by the widespread development of quartz *c*-axis fabrics with central girdles (Kojima & Hide 1958, Wallis *et al.* 1992a,b, Sakagibara *et al.* 1992, Hara *et al.* 1992). Departures from plane-strain are represented by the development of small-circle patterns (e.g. Schmid & Casey 1986). In the following I shall therefore assume the main deformation was plane-strain and equal-area.

There are at least two distinct phases of folding that postdate the phase of orogen-parallel shearing (Hara *et al.* 1977, Faure 1985, Wallis 1990). There is, however, general agreement that the main foliation of the region can be accounted for in terms of one tectonic event, even if some workers locally subdivide this into several different stages (e.g. Hara *et al.* 1990). Formation of the main foliation is, at least in part, synchronous with retrograde metamorphism of the region (Toriumi 1982, Wallis *et al.* 1992a,b).

METHODS OF VORTICITY ANALYSIS

Four different techniques are used to estimate the degree of non-coaxiality of deformation in samples from the Sanbagawa belt. All of the samples underwent penetrative ductile deformation associated with the dominant orogen-parallel shear of the region. Quantitative vorticity analyses of deformed rocks are relatively rare and the consistency of different methods has been little studied. Where possible I have, therefore, used more than one method in a particular sample to estimate the degree of non-coaxiality. The comparable results obtained using different methods suggests that these methods can be used to make quantitative estimates of the rotational component of deformation.

Deformed veins

At any given time during progressive deformation, sectors of material lines that have distinct stretch histories can be defined. Lines that have extended only, shortened only, shortened then extended, and extended then shortened are all possible (e.g. Talbot 1970, Passchier 1990). In natural examples the deformation history of material lines in different orientations may be rep-

resented by the deformation of veins of dykes. These features have been used as strain markers (e.g. Talbot 1970) and to differentiate non-coaxial from coaxial deformation histories (Hutton 1982). Passchier (1990) shows that the orientations of the boundaries between material line sectors with distinct stretch histories can be used to characterize the kinematics of finite deformation by determining finite strain, volume change, and mean vorticity. Wallis (1992a) uses this method to estimate the mean vorticity of a deformed metachert in the south of the Sanbagawa belt (sample A in Fig. 2). The orientation data are given in Wallis (1992a, fig. 6) and suggest $0.51 < W_m < 0.70$.

Vein orientation data can be measured very accurately. There may, however, be some uncertainty about the precise orientation of the sector boundaries. This uncertainty arises because veins may unfold before showing signs of necking or boudinage and they may shorten along their length before folding. The associated uncertainties can be minimized if there is an independent measure of finite strain (Wallis 1992a).

Rotated porphyroclasts

The rotation of rigid objects within a flowing viscous medium is a function of several factors including the degree of non-coaxiality. The relationship between the orientation of such objects and their aspect ratio can be used in vorticity analyses in a variety of geological settings (Passchier 1987, Vissers 1989, Cowan 1990, Wallis *et al.* 1993, Simpson & De Paor 1993). The equations I use in this analysis (Appendix 1) are derived from Ghosh & Ramberg (1976).

The sample material is quartz schist containing abundant large albite porphyroclasts (C in Fig. 2). The porphyroclasts have a well-defined planar internal fabric. In thin-section the trace of this internal fabric lies parallel to the long axes of the porphyroclasts (Fig. 3) suggesting the porphyroclasts grew along a preexisting foliation. Formation of the porphyroclasts and the included fabric predates the dominant deformation during which the porphyroclasts rotated by various amounts. There is no evidence for significant internal deformation of the clasts themselves. Figure 4 shows there is a clear relationship between the orientation of the long axis of the porphyroclasts and their aspect ratio. The data indicate a mean vorticity less than simple shear. Curve fitting using a least squared difference method suggests $0.45 < W_m < 0.60$.

Quartz c-axis fabrics and strain ratio

Quartz-rich tectonites commonly develop crystallographic preferred orientation patterns by slip along particular crystallographic planes. Well-developed *c*-axis fabrics show geometries that can be used to characterize the kinematics of the associated flow (e.g. Lister & Hobbs 1980, Schmid & Casey 1986). In this section I shall follow a number of workers in assuming that the central girdle of a quartz *c*-axis fabric forms perpendicular to the flow plane. This assumption is supported by the following arguments.

For pure shear deformation, theoretical models are in agreement in predicting orthorhombic quartz *c*-axis fabrics with a central girdle perpendicular to the plane of zero finite rotation (e.g. Lister & Hobbs 1980, Wenk *et al.* 1989). This is supported by the observations of Law *et al.* (1984) in naturally deformed samples where there is independent evidence of a very low degree of non-coaxiality. In many natural examples of deformation by simple shear, quartz *c*-axis fabrics are single girdles inclined to the foliation in the direction of shear (Simpson 1981, Schmid & Casey 1986, Law *et al.* 1990). Law *et al.* (1990) give a particularly clear example showing that the *c*-axis girdle and flow plane are perpendicular. These relationships are predicted by the kinematic model of Etchecopar (1977). More sophisticated models based on the Taylor–Bishop–Hill theory have also been used to study the development of quartz *c*-axis fabrics in non-coaxial flow. Lister & Hobbs (1980) emphasize that the leading edge of the fabrics generated in their model is perpendicular to the flow plane. The modelling of Wenk *et al.* (1989) suggests the relationship may be more complex but predict very similar fabrics to those of Lister & Hobbs (1980).

Many quartz *c*-axis fabrics have geometries that are intermediate between those representative of pure and simple shear. Such fabrics commonly have a kinked outline and can most straight-forwardly be interpreted as the result of deformation intermediate between simple and pure shear, i.e. $0 < W_m < 1$ (Law *et al.* 1984, 1986, Platt & Behrmann 1986, Schmid & Casey 1986, Vissers 1989, Wallis 1992a). By analogy with the fabrics developed during progressive simple and pure shearing, it has been suggested that the central girdle of such intermediate fabrics may also form perpendicular to the flow plane (Fig. 5) (Platt & Behrmann 1986, Vissers 1989, Wallis 1992a, Wallis *et al.* 1993).

Under the above assumption, for constant values of L_{ij} the angle between the perpendicular to the central girdle and the flattening plane of finite strain, β, is a function of finite strain and the degree of non-coaxiality. This can be expressed by the following equations:

$$\phi = \tan^{-1}\left\{\frac{\sin 2\beta}{\frac{(R_f+1)}{(R_f-1)} - \cos 2\beta}\right\} \quad (8)$$

$$W_m = \sin\phi\,\frac{(R_f+1)}{(R_f-1)} \quad (9)$$

(Wallis 1992a), where R_f is the strain ratio. Therefore, if β and R_f are known, W_m may be calculated.

Deformed metachert is common in the Sanbagawa belt. The rock type is almost pure quartz and was originally fine-grained making it ideally suited for quartz fabric studies. Quartz *c*-axis fabrics that developed during the orogen-parallel shear have been measured throughout central Shikoku (Kojima & Hide 1958, Wallis *et al.* 1992 a,b, Hara *et al.* 1992, Sakagibara *et al.*

1992). The majority of these fabrics suggest that regional deformation was intermediate between simple and pure shear.

In three samples (A, C and D in Fig. 2) with well-defined quartz *c*-axis fabrics it was possible to estimate both the angle between the flow plane and the flattening plane and the aspect ratio of the strain ellipse (Figs. 6 and 7). Using equations (8) and (9) the degree of non-coaxiality, W_m, can therefore be determined in these samples. The three estimates are: sample A, $0.35 < W_m < 0.60$; sample C, $0 < W_m < 0.5$; sample D, $0.66 < W_m < 0.74$. In the samples A and C the quartz *c*-axis fabrics are in agreement with the estimates of W_m using different methods. In all cases the results show a significant departure from simple shear. The fourth sample shown in Fig. 6, sample B, is discussed in the following section.

Oblique grain shape and quartz c-axis fabrics

In two-dimensional flow, if α is the acute angle between lines of zero instantaneous rotation (the flow apophyses) and theta is the acute angle between these lines and the instantaneous stretching axes, ISA (see fig. 1, Passchier 1988b), then:

$$W_n = \cos \alpha \tag{10}$$

(e.g. Passchier 1988b). Also,

$$\theta = \tfrac{1}{2}(90° - \alpha) \tag{11}$$

therefore

$$W_n = \sin 2\theta. \tag{12}$$

In the previous section I have argued that the orientation of the flow plane may be estimated from the geometry of well-developed quartz *c*-axis fabrics. If the orientation of ISA can also be determined, equation (12) can be used to find W_n.

Grain-shape fabrics oblique to the main foliation are observed in many metamorphic tectonites and have been produced in laboratory experiments (Ree 1991). Such fabrics form by progressive stretching and rotation of dynamically recrystallizing grains which is, however, modified by the process of grain boundary migration (Means 1981, Lister & Snoke 1984, Knipe and Law 1987). During the last increment of deformation new grains will be stretched in the direction of maximum instantaneous stretching parallel to the ISA that is extending. Other grains will have rotated by greater or lesser amounts towards the flattening plane of finite strain and have been modified by recrystallization and grain boundary migration. It should therefore be possible to identify the approximate orientation of ISA by taking the highest angle to the foliation of the new oblique grain shape fabric. In order for the long axes of recrystallized grains to rotate progressively away from ISA they have to be equant at the time of formation. This is unlikely to be precisely true. However, support for this method is given by observations in a sample naturally deformed by simple shear (Law *et al.* 1990). In this sample the observed oblique grain shape fabric has a maximum angle of 44° to the shear plane. This is only 1° different from the predicted angle between the flow apophysis and ISA during simple shear of 45°.

The above type of analysis can be carried out in samples where there are well-developed *c*-axis and oblique grain shape fabrics. Two such samples (samples A and B) were located in the present study (Fig. 8). The angle between the perpendicular to the central girdle of the *c*-axis and the orientation of the maximum of the grain shape fabric can be used to estimate W_n. The orientation data relating to the oblique grain shape fabric in samples A and B are given in Fig. 9 and the results give sample A $0.72 < W_n < 0.81$; sample B $0.9 < W_n < 0.97$.

If deformation was steady state then the value for W_n can be used with the angle β to calculate R_f. The results can be derived from the standard solution of a quadratic equation

$$R_f = \frac{-b \pm \sqrt{b^2 - 4ac}}{2a}, \tag{13}$$

where:

$$a = 2W_m^2 - 2W_m^2 \cos 2\beta - \sin^2 2\beta$$
$$b = -2 \sin^2 2\beta$$
$$c = 2W_m^2 + 2W_m^2 \cos 2\beta - \sin^2 2\beta$$

(Appendix 2). Using the above values suggests for sample B, $33 > R_f > 8$. The same calculation for sample A gives an estimate for R_f over twice the measured value. Similar estimates of W_m were obtained from the same sample using deformed veins and quartz *c*-axis fabric. Both these features are likely to have formed over a greater part of the deformation history than the recrystallized grain shape fabric and are therefore more representative of W_m. The discrepancy with the result from the grain shape fabric suggests that in this sample, W_n during the final increment of deformation was somewhat greater than W_m, the mean vorticity.

CONTRADICTORY SENSE OF SHEAR INDICATORS AND GENERAL SHEAR

One of the characteristics of general (sub-simple) shear (Simpson & De Paor 1993) is that rotations of material lines and rigid objects may be opposite to the bulk sense of shear. The potential for rotations of either direction during general non-coaxial deformation is, for instance, illustrated by the calculations of Ghosh & Ramberg (1976). In the higher grade parts of the Sanbagawa belt porphyroclasts are commonly present which have overgrown a metamorphic fabric and subsequently been rotated. Both senses of rotation are locally present in the same sample (Wallis 1992b, fig. 3). Another important effect of general shear is the potential for the development of conjugate shears with opposed senses of shear (Platt 1984, Bobyarchick 1986, Simpson & De Paor 1993).

The initiation of shear bands requires strain softening

Fig. 3. Photomicrograph of albite porphyroclast used in vorticity analysis (sample C garnet–biotite–quartz schist). The long axis of the porphyroclast lies parallel to the trace of a preexisting foliation defined by inclusion trails (Wallis *et al.* 1992a).

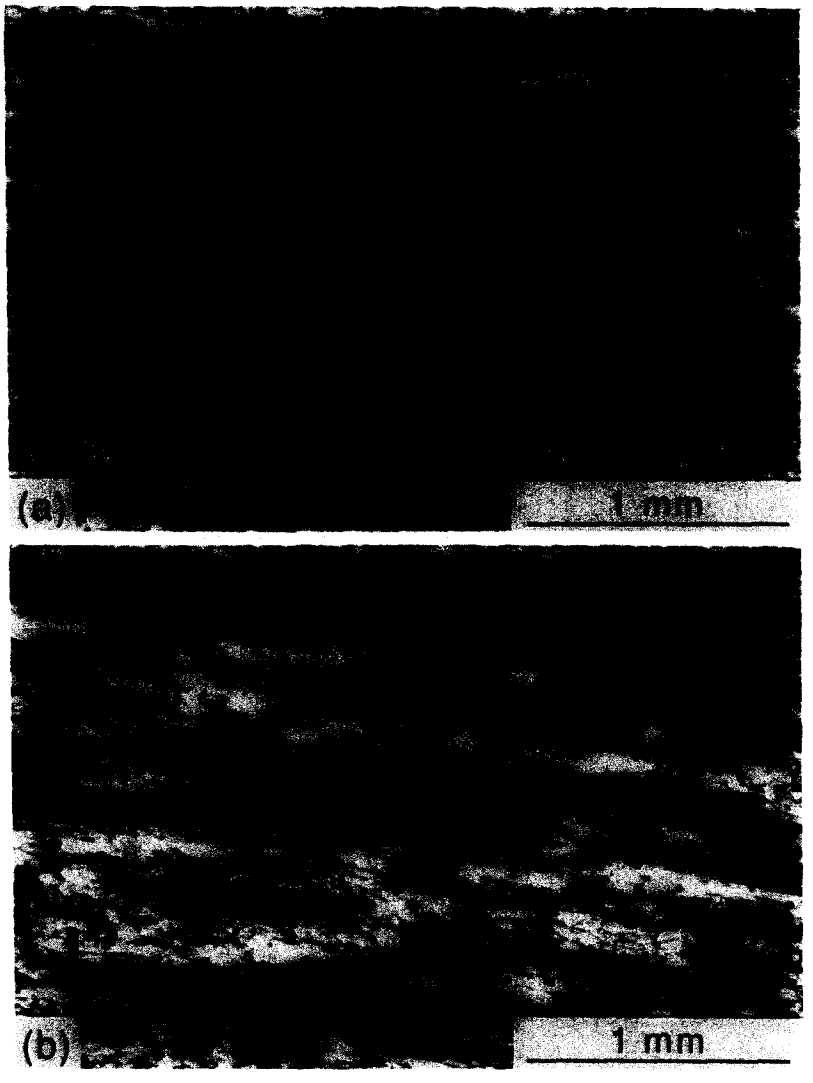

Fig. 8. Photomicrographs of the oblique grain shape fabrics: (a) sample A, (b) sample B. Samples for which there was microstructural evidence for post-deformational annealing were not included in the study. In both cases the mesoscopic foliation is approximately parallel to the base of the photograph.

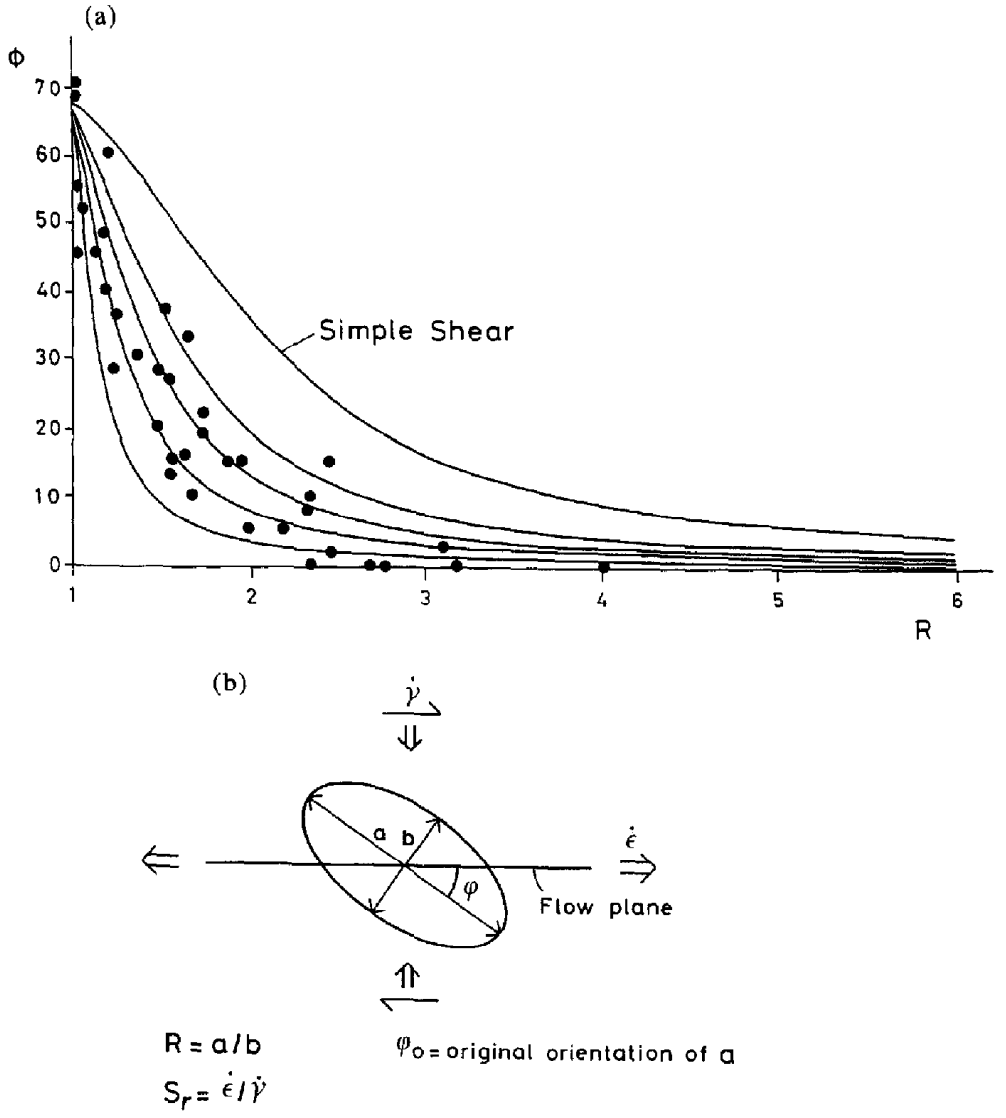

Fig. 4. (a) Plot of aspect ratio against rotation angle of porphyroclasts for sample C and the predicted relationship for different W_m values. Curves are for $W_m = 0.2, 0.4, 0.6, 0.8, 1.0$. There is a clear deviation from the expected relationship for simple shear suggesting $0.45 > W_m > 0.60$, $5.5 > R_f > 5.8$. All porphyroclasts used in the study have a consistent angular relationship between the long axis of the porphyroclasts and the trace of the inclusion fabric suggesting they originated in approximately the same orientation. The earlier fabric may not have been parallel to the present foliation but an original angle of up to 20° makes no significant difference to the results. The porphyroclasts lack undulose extinction and subgrains suggesting there was no significant internal deformation. (b) Definition of symbols used in the rotation analysis of (a) and in Appendix 1.

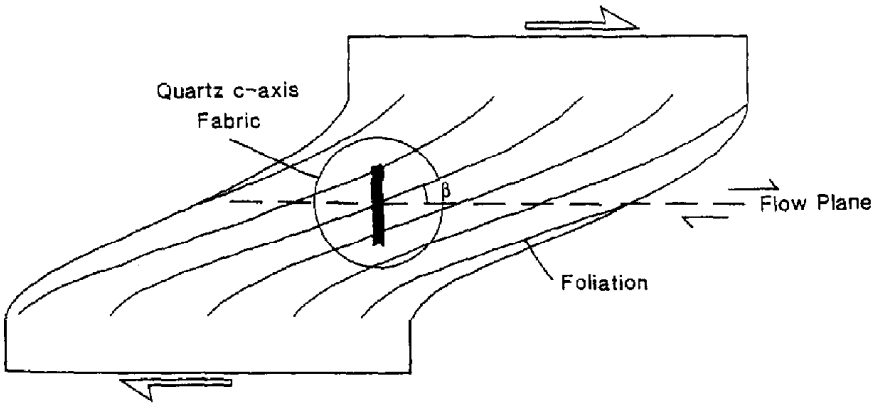

Fig. 5. Illustration of the relationship between the central girdle of a quartz *c*-axis fabric and the flow plane. This angle is defined as β and used in the vorticity analysis discussed in the text. The angle β can be plotted in the Mohr circle for stretch as shown in Fig. A1.

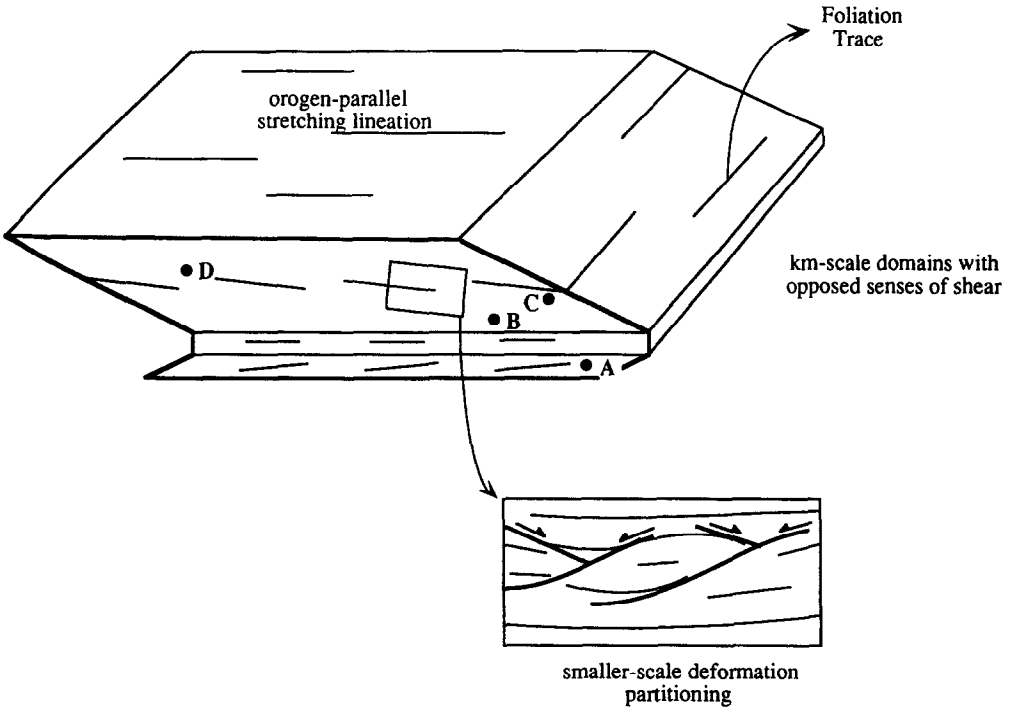

Fig. 10. Block diagram showing the way in which deformation is partitioned into domains with opposed senses of shear in central Shikoku. The diagram is schematic but represents a package of material approximately 6 km thick. The effects of late-stage folding have been omitted for simplicity. The inset shows localized shear band development on the metre to centimetre scale. More data are required to determine the lateral geometries of the large-scale shear zones with opposed senses of shear. The front face of the block diagram represents the plane of study for the vorticity analyses. The structural levels and relative positions of the samples A, B, C and D are also indicated.

observation for these studies is roughly parallel to the trend of the belt (e.g. Toriumi 1982, Faure 1985, Wallis *et al.* 1992a) and therefore close to horizontal (Fig. 10). The flow plane of the orogen-parallel shear in the Sanbagawa belt must therefore also be close to horizontal and the shortening across this plane must cause thinning of the tectonic pile.

The amount of thinning depends on both the value of W_m and the finite strain. Assuming time constant behaviour, the equation relating these quantities to the stretch along the flow plane (A_1) is:

$$A_1 = \tfrac{1}{2}(1 - W_m^2)^{1/2}\left[\left(R_f + R_f^{-1} + 2\frac{(1 + W_m^2)}{1 - W_m^2}\right) + (R_f + R_f^{-1} - 2)^{1/2}\right] \quad (14)$$

(Wallis *et al.* 1993) (Appendix 2). This equation can be used to relate the amount of thinning for a given finite strain and constant vorticity (Fig. 12). The results from this study suggest a thinning of 35–65%.

IMPLICATIONS FOR TECTONICS OF THE SANBAGAWA BELT

The quantitative analysis of strain and vorticity in central Shikoku suggests that the region underwent ductile extension and thinning of the order of 50%. This ductile deformation is related to shearing in a dominantly E–W direction and began close to the peak of metamorphic conditions (Hara *et al.* 1990, Wallis *et al.* 1992b) which in the high-grade regions of central Shikoku represent depths of 30 km or more (Banno & Sakai 1989, Enami 1982, Enami *et al.* 1994). A value of 50% for the ductile extension can, therefore, account for around 15 km of the exhumation of this region. At such levels in the crust it is likely that brittle deformation

Fig. 11. Strain compatibility requirements shown in two dimensions for parallel zones with opposed senses of shear. If the non-coaxial zones are simple shear (a) then the bounding domain has to be a zone of no deformation. However, if the non-coaxial zones are general (sub-simple) shear (b), then the bounding domain can be one of pure shear. Only in the second case can a foliation be developed throughout the sequence as is observed in central Shikoku. The numbers I, II and III refer to three domains with distinct deformational histories. The diagrams show the same state of finite strain in all the non-coaxial domains. Deformation in domains I and III of (b) has a value of $W_m = 0.5$ and stretch of 2 along the boundary with domain II. The orientation and shape of the strain ellipse is shown in domain I of both (a) & (b). Deformation in each of the domains I, II and III is also shown by a series of Mohr circles for the reciprocal stretch tensor, H_{ij} (e.g. Means 1983). Strain compatibility requires that the Mohr circle for domain II has to pass through the intersection of the Mohr circles for domains I and III. If the deformation of domains I and III is simple shear then there is only one point of intersection representing zero deformation. The stretch and rotation of lines a, b and c in the block diagrams are represented by points on the Mohr circles.

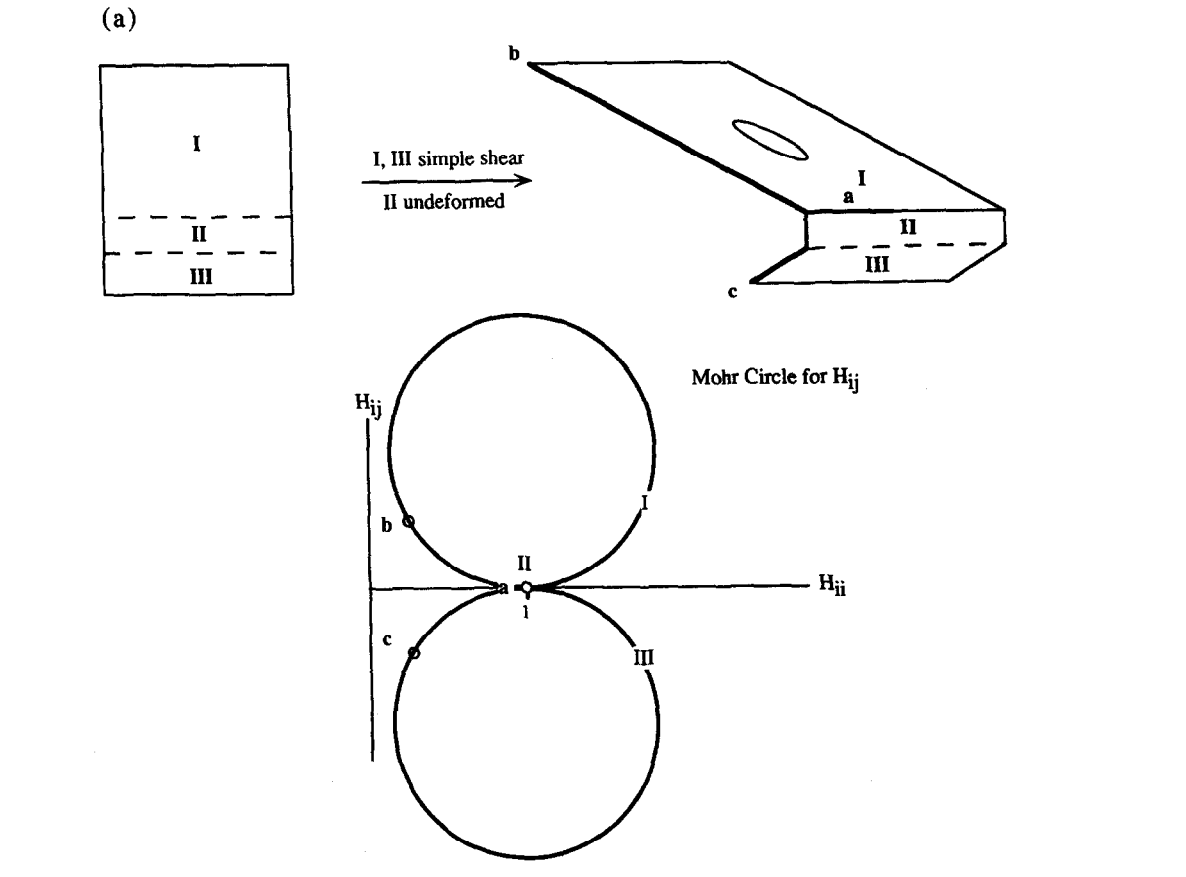
(a)
I
II
III
I, III simple shear
II undeformed
b
I
a
II
III
c
Mohr Circle for H_{ij}
H_{ij}
b
I
II
a
1
H_{ii}
c
III

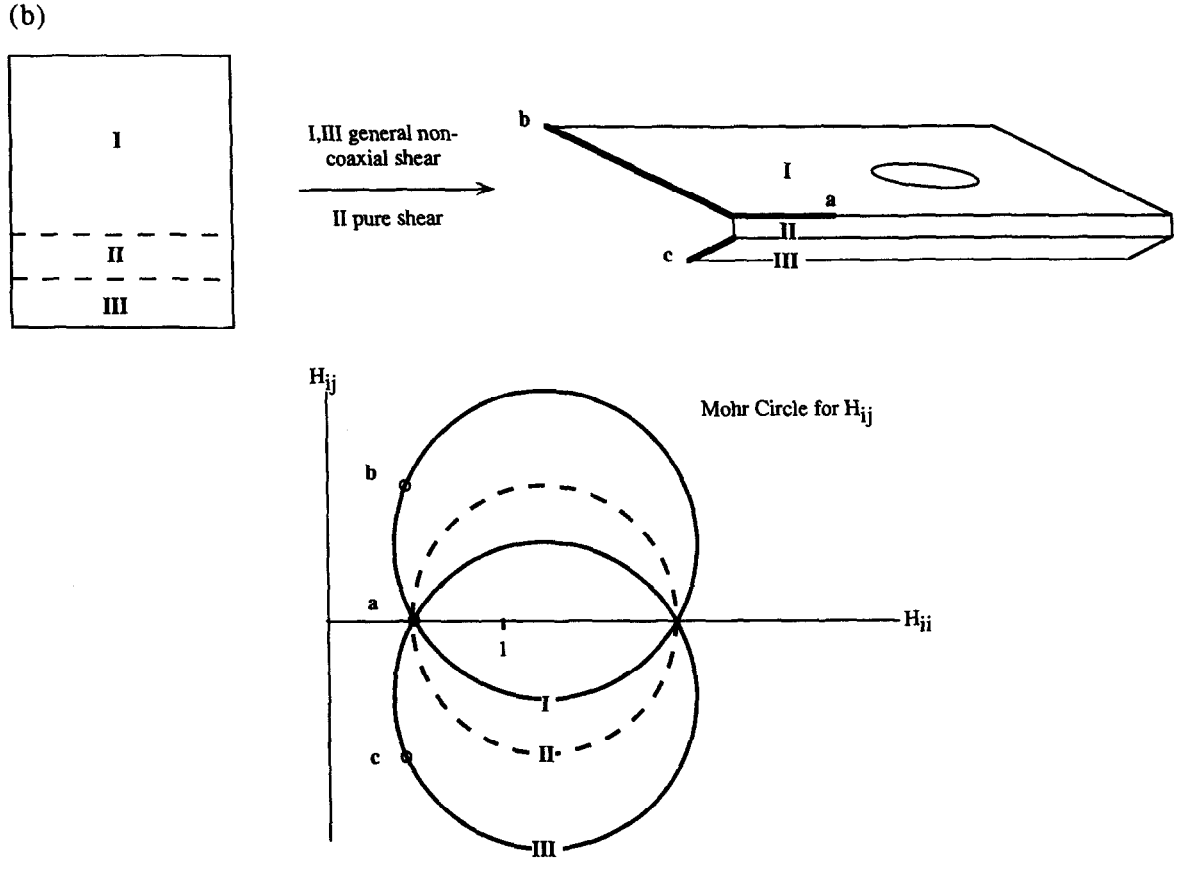
(b)
I
II
III
I,III general non-coaxial shear
II pure shear
b
I
a
II
c
III
H_{ij}
Mohr Circle for H_{ij}
b
a
1
H_{ii}
I
II
c
III

Fig. 11.

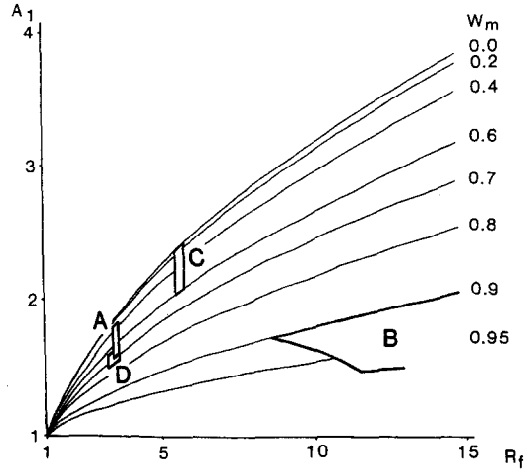

Fig. 12. Graph showing the relationship between R_f and amount of stretch along the flow plane for different values of W_m. The thinning perpendicular to the flow plane is simply the inverse. The curves are drawn using equation (16) which is derived in Appendix 2. When deformation is close to simple shear changes in W_m imply greater changes in the associated amount of shortening perpendicular to the flow plane than when deformation is close to pure shear. In the present study the estimates for W_m cover a relatively large range. The associated finite strain is, however, also different and the resulting estimates of thinning perpendicular to the flow plane lie between 35 and 60%.

would become dominant and any further tectonic thinning would probably be by movement along normal faults. Such faults would have the property of extending along their length as they propagated (e.g. Means 1989). Locally candidates for such low-angle extensional faults between the Sanbagawa belt and its former hangingwall material have been identified (Wallis *et al.* 1990).

The mechanical analysis of Platt (1986) suggests that extension perpendicular to convergent margins may be an important process in the exhumation of coherent high *P–T* metamorphic terrains. Such a model cannot, however, account for the orogen-parallel shear and associated thinning of the Sanbagawa belt. Several workers have suggested the orogen-parallel shearing of the Sanbagawa belt is likely to be related to oblique convergence (e.g. Faure 1985, Toriumi & Noda 1986). Oblique convergence may be able to account for the orogen-parallel shearing; by itself, however, it cannot account for the tectonic thinning of the Sanbagawa belt. A possible mechanism for explaining both the orogen-parallel movements and the tectonic thinning is extension of the forearc region produced during oblique convergence when the strike-slip component of movement changes along strike (e.g. McCaffrey 1992). This may occur, for instance, when the subducting plate has a pole of rotation close to the convergent margin. Plate reconstructions of the East-Asian continental margin suggest that at the time of formation of the Sanbagawa metamorphism the Izanagi plate was subducting below the area with a nearby pole of rotation (Engebretson *et al.* 1985). A more detailed study of the role of oblique subduction in the tectonics of the Sanbagawa belt is in preparation.

CONCLUSIONS

Vorticity analysis can help characterize the kinematics of regional deformation particularly in regions of penetrative ductile shear. Knowledge of the kinematic type of deformation can in turn be used to test possible tectonic interpretations. In the Sanbagawa metamorphic belt indicators of the degree of non-coaxiality suggest that the main penetrative deformation of the region was a general non-coaxial type which caused major ductile extension. Quantitative estimates of finite-strain and the degree of non-coaxiality suggest that the tectonic pile was thinned by an order of 50%. The association of orogen-parallel shear in the Sanbagawa belt with ductile extension shows that this developed during exhumation of the region and is not simply related to subduction. The combination of orogen-parallel shear and ductile thinning may be related to oblique subduction by a plate with a pole of rotation close to the former convergent margin.

Acknowledgements—I thank Shohei Banno for first introducing me to the geology of the Sanbagawa belt and the participants of the Penrose conference for stimulating discussions on vorticity analysis. Constructive reviews by Basil Tikoff and Declan De Paor as well as the editing of Win Means and Sue Treagus were all very helpful in revising parts of this paper. I also thank my friends and colleagues at CCF, in particular Rémi Soula, for encouraging me to complete this work. Sample D was collected by Takao Hirajima. This work was carried out during the tenure of fellowships from the Royal Society/JSPS and the European Commission. Additional support was given by the British Council.

REFERENCES

Banno, S. 1964. Petrologic studies on the Sanbagawa crystalline schists in the Bessi-Ino district, central Shikoku, Japan. *J. Fac. Sci., Univ. Tokyo, Sec.* 2, **15**, 203–319.

Banno, S. & Sakai, C. 1989. Geology and metamorphic evolution of the Sanbagawa belt, Japan. In: *Evolution of Metamorphic Belts* (edited by Daly, J. S., Cliff, R. A. & Yardley, B. W. D.). *Spec. Pub. geol. Soc. Lond.* **43**, 519–532.

Bell, T. H. & Cuff, C. 1989. Dissolution, solution transfer, diffusion versus fluid flow and volume loss during deformation/metamorphism. *J. Met. Geol.* 7, 425–447.

Bobyarchick, A. R. 1986. The eigenvalues of steady flow in Mohr space. *Tectonophysics* **122**, 35–51.

Cowan, D. 1990. Kinematic analysis of shear zones in sandstone and mudstone of the Shimanto belt, Shikoku, SW Japan. *J. Struct. Geol.* **12**, 431–441.

De Paor, D. G. & Means, W. D. 1984. Mohr circles of the First and Second Kind and their use to represent tensor operations. *J. Struct. Geol.* **6**, 693–701.

Durney, D. W. 1972. Solution transfer, an important geological deformation mechanism. *Nature* **235**, 315–317.

Elliott, D. 1972. Deformation paths in structural geology. *Bull. geol. Soc. Am.* **83**, 2621–2638.

Engebretson, D. C., Cox, A. & Gordon, R. G. 1985. Relative motions between oceanic and continental plates in the Pacific basin. *Spec. Pap. geol. Soc. Am.* **59**.

England, P. & Houseman, G. 1988. The mechanics of the Tibetan plateau. *Phil. Trans. R. Soc. Lond. Ser. A* **326**, 301–320.

Enami, M. 1982. Oligoclase biotite zone of the Sanbagawa metamorphic terrain in the Bessi district, central Shikoku. *J. geol. Soc. Japan* **88**, 857–900.

Enami, M., Wallis, S. R. & Banno, Y. 1994. Paragenesis of sodic pyroxene-bearing quartz schists: implications for the P–T history of the Sanbagawa belt. *Contrib. Min. Pet.* **116**, 182–198.

Etchecopar, A. 1977. A plane kinematic model of progressive deformation in a polycrystalline aggregate. *Tectonophysics* **39**, 121–139.

Faure, M. 1983. Eastward ductile shear during the early tectonic phase in the Sanbagawa belt. *J. geol. Soc. Japan* **89**, 319–329.

Faure, M. 1985. Microtectonic evidence for eastward ductile shear in the Jurassic orogen of S.W. Japan. *J. Struct. Geol.* **7**, 175–186.

Fisher, N. I., Lewis, T. & Embleton, B. J. J. 1987. *Statistical Analysis of Spherical Data*. Cambridge University Press.

Ghosh, S. K. 1987. Measure of non-coaxiality. *J. Struct. Geol.* **9**, 111–113.

Ghosh, S. K. & Ramberg, H. 1976. Reorientation of inclusions by combination of pure and simple shear. *Tectonophysics* **34**, 1–70.

Gratier, J. P. 1982. Estimation of volume changes by comparative chemical analyses in heterogeneously deformed rocks (folds with mass transfer). *J. Struct. Geol.* **5**, 329–339.

Hara, I., Hide, K., Takeda, K., Tsukuda, E., Tokuda, M. & Shioda T. 1977. Tectonic movement in the Sanbagawa Belt. In: *The Sanbagawa Belt* (edited by Hide, K.). Hiroshima University Press, 307–390.

Hara, I., Shiota, T., Okamoto, K., Takeda, K., Hayasaka, Y. & Sakurai, Y. 1990. Nappe structure of the Sanbagawa belt. *J. Met. Geol.* **8**, 441–456.

Hara, I., Shiota, T., Hide, K., Kanai, K., Goto, M., Seki, S., Kaikiri, K., Takeda, K., Hayasaka, Y., Miyamoto, T., Sakurai, Y. & Ohmoto, Y. 1992. Tectonic evolution of the Sambagawa schists and its implications in convergent margin processes. *J. Hiroshima Univ. Ser. C* **9**, 495–595.

Hara, I., Shiota, T., Takeda, K., Okamoto, K. & Hide, K. 1990. Sanbagawa terrane. In: *Pre-Cretaceous Terranes of Japan* (edited by Ichikawa, K., Mizutani, S., Hara, I., Hada, S. & Yao, A.). *Pre-Jurassic Evolution of Eastern Asia, IGCP Project No.* **224**, 137–163.

Harris, L. B. & Cobbold, P. R. 1985. Development of conjugate shear bands during bulk simple shearing. *J. Struct. Geol.* **7**, 37–44.

Higashino, T. 1990. The higher grade metamorphic zonation of the Sambagawa metamorphic belt in central Shikoku, Japan. *J. Met. Geol.* **8**, 413–423.

Hutton, D. H. W. 1982. A tectonic model for the emplacement of the main Donegal granite, NW Ireland. *J. geol. Soc. Lond.* **139**, 615–631.

Jolivet, L., Dubois, R., Fournier, M., Goffe, B., Michard, A. & Jourdan, C. 1990. Ductile extension in Alpine Corsica. *Geology* **18**, 1007–1010.

Kerrich, R., Beckinsale, R. D. & Durham, J. J. 1977. The transition between deformation regimes dominated by intercrystalline diffusion and intracrystalline creep evaluated by oxygen isotope geothermometry. *Tectonophysics* **38**, 241–258.

Knipe, R. J. & Law, R. D. 1987. The influence of crystallographic orientation and grain boundary migration on microstructural and textural evolution in an *S–C* mylonite. *Tectonophysics* **135**, 155–169.

Kojima, G. & Hide, K. 1958. Kinematic interpretation of the quartz fabric of triclinic tectonites from Besshi, Central Shikoku. Japan. *J. Fac. Sci., Hiroshima Ser. C* **2**, 195–226.

Law, R. D., Casey, M. & Knipe, R. J. 1986. Kinematic and tectonic significance of microstructures and crystallographic fabrics within quartz mylonites from Assynt and Eriboll regions of the Moine thrust zone, NW Scotland. *Trans. R. Soc. Edin.* **77**, 99–125.

Law, R. D., Knipe, R. J. & Dayan, H. 1984. Strain path partitioning within thrust sheets: microstructural and petrofabric evidence from the moine thrust zone at loch Eriboll, northwest Scotland. *J. Struct. Geol.* **6**, 477–497.

Law, R. D., Schmid, S. M. & Wheeler, J. 1990. Simple shear deformation and quartz crystallographic fabrics: a possible natural example from the Torridon area of NW Scotland. *J. Struct. Geol.* **12**, 29–45.

Lister, G. S. & Hobbs, B. E. 1980. The simulation of fabric development during plastic deformation and its application to quartzite: the influence of deformation history. *J. Struct. Geol.* **2**, 355–370.

Lister, G. S. & Snoke, A. W. 1984. *S–C* mylonites. *J. Struct. Geol.* **6**, 617–639.

Lister, G. S. & Williams, P. F. 1983. The partitioning of deformation in flowing rock masses. *Tectonophysics* **92**, 1–33.

Malvern, L. E. 1969. *Introduction to the Mechanics of a Continuous Medium*. Prentice-Hall, Englewood Cliffs, New Jersey.

McCaffrey, R. 1992. Oblique plate convergence, slip vectors, and forearc deformation. *J. geophs. Res.* 97, 8905–8915.

McKenzie, D. P. 1979. Finite deformation during fluid flow. *Geophs. J. R. astr. Soc.* **58**, 689–715.

Means, W. D. 1981. The concept of steady state foliation. *Tectonophysics* **78**, 179–199.

Means, W. D. 1982. An unfamiliar Mohr circle construction for finite strain. *Tectonophysics* **89**, T1–T6.

Means, W. D. 1983. Application of the Mohr-circle construction to problems of inhomogeneous deformation. *J. Struct. Geol.* **5**, 279–286.

Means, W. D. 1989. Stretching faults. *Geology* **17**, 893–896.

Means, W. D., Hobbs, B. E., Lister, G. S. & Williams, P. F. 1980. Vorticity and non-coaxiality in progressive deformations. *J. Struct. Geol.* **2**, 371–378.

Molnar, P. & Tapponier, P. 1978. Active tectonics of Tibet. *J. geophys. Res.* **832**, 5361–5375.

O'Hara, K. 1990. State of strain in mylonites from the western Blue Ridge province, southern Appalachians: the role of volume loss. *J. Struct. Geol.* **12**, 419–430.

Passchier, C. W. 1984. The generation of ductile and brittle shear bands in a low-angle mylonite zone. *J. Struct. Geol.* **6**, 273–281.

Passchier, C. W. 1987. Stable positions of rigid objects in non-coaxial flow—a study in vorticity analysis. *J. Struct. Geol.* **9**, 679–690.

Passchier, C. W. 1988a. Analysis of deformation paths in shear zones. *Geol. Rdsch.* **77**, 309–318.

Passchier, C. W. 1988b. The use of Mohr circles to describe non-coaxial progressive deformation. *Tectonophysics* **149**, 323–338.

Passchier, C. W. 1990. Reconstruction of deformation and flow parameters using deformed vein sets. *Tectonophysics* **180**, 185–199.

Platt, J. P. 1984. Secondary cleavages in ductile shear zones. *J. Struct. Geol.* **6**, 439–442.

Platt, J. P. 1986. Dynamics of orogenic wedges and the uplift of high pressure metamorphic rocks. *Bull. geol. Soc. Am.* **97**, 1037–1053.

Platt, J. P. & Behrmann, J. H. 1986. Structures and fabrics in the crustal-scale shear zone. Betic Cordillera, SE Spain. *J. Struct. Geol.* **8**, 15–33.

Platt, J. P. & Vissers, R. L. M. 1980. Extensional structures in anisotropic rocks. *J. Struct. Geol.* **2**, 397–410.

Ramsay, J. G. & Huber, M. I. 1983. *The Techniques of Modern Structural Geology, Volume* 1: *Strain Analysis*. Academic Press, New York.

Ree, J.-H. 1991. An experimental steady state foliation. *J. Struct. Geol.* **13**, 1001–1012.

Royden, L. & Burchfiel, B. C. 1987. Thin-skinned extension within the convergent Himalayan region: gravitational collapse of a Miocene topographic front. *Spec. Pub. geol. Soc. Lond.* **28**, 611–619.

Rutter, E. H. 1983. Pressure solution in nature, theory and experiment. *J. geol. Soc. Lond.* **140**, 725–740.

Sakagibara, N., Hara, I., Kanai, K., Kaikiri, K., Shiota, T., Hide, K. & Paulitsch, P. 1992. Quartz microtextures of the Sambagawa schists and their implications in convergent margin processes. *The Island Arc* **1**, 186–197.

Schmid, S. M. & Casey, M. 1986. Complete fabric analysis of some commonly observed quartz c-axis patterns. In: *Mineral and Rock Deformation: Laboratory Studies—The Paterson Volume* (edited by Hobbs, B. E. & Heard, H. C.). *Am. Geophys. Un. Geophys. Monogr.* **36**, 263–286.

Selverstone, J. 1985. Petrologic constraints on imbrication, metamorphism, and uplift in the SW Tauern Window, eastern Alps. *Tectonics* **4**, 687–704.

Selverstone, J. 1988. Evidence for east–west crustal extension in the eastern Alps: implications for the unroofing history of the Tauern Window. *Tectonics* **7**, 87–105.

Shimizu, I. 1988. Ductile deformation in the low-grade part of the Sanbagawa metamorphic belt in the northern Kanto mountains, central Japan. *J. geol. Soc. Japan* **94**, 609–628.

Simpson, C. 1981. Ductile shear zones: a mechanism for rock deformation in the orthogneisses of the Maggia nappe, Ticino. Unpublished Ph.D. thesis, ETH, Zurich.

Simpson, C. & De Paor D. 1993. Strain and kinematic analysis in general shear zones. *J. Struct. Geol.* **15**, 1–20.

Takasu, A., Wallis, S. R., Banno, S. & Dallmeyer, R. D. 1994. Evolution of the Sanbagawa metamorphic belt. *Lithos* **33**, 119–134.

Talbot, C. J. 1970. The minimum strain ellipsoid using deformed quarts veins. *Tectonophysics* **9**, 46–76.

Tikoff, B. & Fossen, H. 1993. Simultaneous pure and simple shear: the unifying deformation matrix. *Tectonophysics* **217**, 267–283.

Toriumi, M. 1982. Stress strain and uplift. *Tectonics* **1**, 57–72.

Toriumi, M. 1989. Microstructures of regional metamorphic rocks. In: *Rheology of Solids and of the Earth* (edited by Karato, S. & Toriumi, M.). Oxford University Press, 319–337.

Toriumi, M. & Noda, H. 1986. The origin of strain patterns resulting from contemporaneous deformation and metamorphism in the Sanbagawa metamorphic belt. *J. Met. Geol.* **4**, 409–420.

Truesdell, C. 1954. *The Kinematics of Vorticity*. Indiana University Press, Bloomington, Indiana.

Vissers, R. L. M. 1989. Asymmetric quartz *c*-axis fabrics and flow vorticity: a study using rotated garnets. *J. Struct. Geol.* **11**, 231–244.

Wallis, S. R. 1990. The timing of folding and stretching in the Sanbagawa belt, the Asemigawa region, central Shikoku. *J. geol. Soc. Japan* **96**, 345–352.
Wallis, S. R. 1992a. Vorticity analysis in a metachert from the Sanbagawa belt, SW Japan. *J. Struct. Geol.* **14**, 271–280.
Wallis, S. R. 1992b. Do smoothly curved, spiral-shaped inclusion trails signify porphyroblast rotation?—Comment. *Geology* **20**, 1054–1055.
Wallis, S. R. & Banno, S. 1990. The Sanbagawa belt—trends in research. *J. Met. Geol.* **8**, 393–399.
Wallis, S. R., Banno, S. & Radvanec, M. 1992a. Kinematics, structure, and relationship to metamorphism of the east–west flow in the Sanbagawa belt, southwest Japan. *The Island Arc* **1**, 176–185.
Wallis, S. R., Enami, M., Takasu, A., Banno, S. & Ikeda, T. 1992b. Paired metamorphic belts in southwest Japan. *29th IGC excursion guides, Spec. Publ. geol. Soc. Japan*, 133–169.
Wallis, S. R., Hirajima, T. & Yanai, S. 1990. Sense and direction of movement along the Atokura fault at Shimonita, Kanto Mountains. *J. geol. Soc. Japan* **96**, 977–980.
Wallis, S. R., Platt, J. P. & Knott, S. D. 1993. Recognition of synconvergence extension in accretionary wedges with examples from the Calabrian Arc and the Eastern Alps. *Am. J. Sci.* **293**, 463–495.
Wenk, H.-R., Canova, G., Molinari, A. & Kocks, U. F. 1989. Viscoelastic modeling of texture development in quartzite. *J. geophs. Res.* **94**, 17,895–17,906.
Wright, T. O. & Platt, L. B. 1982. Pressure dissolution and cleavage in the Martinsburg shale. *Am. J. Sci.* **282**, 122–135.

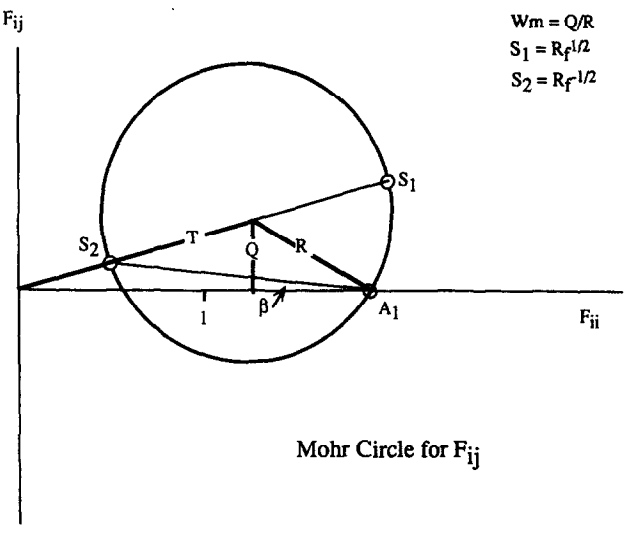

Fig. A1. Mohr circle in stretch space representing the position gradients tensor F_{ij} (e.g. Passchier 1988a,b). For equal volume deformation T and R are defined by the finite strain. The height of the circle above the horizontal axis, Q, is a function of both the finite strain and W_m. This construction can be used to derive the relationships given by equations (15) and (16).

APPENDIX 1

In this paper I have chosen to define the angle used in the study of rotated porphyroclasts as the angle between the long axis of the rigid object and the flow plane. The symbols used in this analysis are defined in Fig. 4(b). The equations used to generate curves in Fig. 4(a) are derived from the work by Ghosh & Ramberg (1976) by substituting $\phi = \phi - 90°$ in their equations (1) and (2) as follows.

After substitution, equation (1) of Ghosh & Ramberg (1976) becomes:

$$\dot{\phi} = \dot{\varepsilon}_x \frac{(R^2-1)}{(R^2+1)} \sin 2(\phi - 90)$$

$$\dot{\phi} = -\dot{\varepsilon}_x \frac{(R^2-1)}{(R^2+1)} \sin 2\phi. \quad \text{(A1)}$$

Equation (2) is then:

$$\dot{\phi} = \dot{\gamma} \frac{[R^2 \cos^2(\phi - 90) + \sin^2(\phi - 90)]}{(R^2+1)}$$

$$\dot{\phi} = \dot{\gamma} \frac{(R^2 \sin^2\phi + \cos^2\phi)}{(R^2+1)}. \quad \text{(A2)}$$

These are the expressions giving the rate of rotation of a rigid ellipse in a viscous fluid for pure and simple shearing, respectively. Addition of the two gives the rotation rate for a combination of simple and pure shearing, i.e. general (sub-simple) shearing. Therefore

$$\dot{\phi} = \dot{\gamma} \frac{(R^2 \sin^2\phi + \cos^2\phi)}{(R^2+1)} - \dot{\varepsilon}_x \frac{(R^2-1)}{(R^2+1)} \sin 2\phi$$

which after rearrangement gives

$$\dot{\phi} = \dot{\gamma}[\mathrm{A} \cos^2\phi + \mathrm{B} \sin^2\phi + \mathrm{C} \sin^2\phi] \quad \text{(A3)}$$

where,

$$\mathrm{A} = \frac{1}{(R^2+1)}; \quad \mathrm{B} = -S_r \frac{(R^2-1)}{(R^2+1)}; \quad \mathrm{C} = \frac{R^2}{(R^2+1)}; \quad \text{and} \quad S_r = \frac{\dot{\varepsilon}_x}{\dot{\gamma}}$$

Equation (A3) can be arranged to give

$$\int_0^{\gamma} d\gamma = \int_{\phi_0}^{\phi} \frac{d\phi}{\left(\frac{\mathrm{A}+\mathrm{C}}{2}\right) + \left(\frac{\mathrm{A}-\mathrm{C}}{2}\right) \cos 2\phi + \mathrm{B} \sin 2\phi} \quad \text{(A4)}$$

where ϕ_0 is the original angle of the long axis of the object. The right-hand side is now in the form of a standard integral for which a solution can be found in reference tables. Integrating between 0 and γ and between ϕ_0 and ϕ and solving for ϕ gives the following results (given in the same form as Ghosh & Ramberg 1976),

(1) If $S_r < \dfrac{R}{(R^2-1)}$ then,

$$\phi = \arctan\left\{\frac{(\mathrm{AC}-\mathrm{B}^2)^{1/2}}{\mathrm{C}} \tan\left[\gamma(\mathrm{AC}-\mathrm{B}^2)^{1/2} + \arctan\left(\frac{\mathrm{B}+\mathrm{C}\tan\phi_0}{(\mathrm{AC}-\mathrm{B}^2)^{1/2}}\right)\right] - \frac{\mathrm{B}}{\mathrm{C}}\right\}. \quad \text{(A5)}$$

(2) If $S_r > \dfrac{R}{(R^2-1)}$ then,

$$\phi = \arctan\left\{\frac{\mathrm{P}[\mathrm{B} + (\mathrm{B}^2-\mathrm{AC})^{1/2}] - \mathrm{B} + (\mathrm{B}^2-\mathrm{AC})^{1/2}}{\mathrm{C}(1-\mathrm{P})}\right\} \quad \text{(A6)}$$

where

$$P = \frac{\mathrm{B}+\mathrm{C}\tan\phi_0 - (\mathrm{B}^2-\mathrm{AC})^{1/2}}{\mathrm{B}+\mathrm{C}\tan\phi_0 + (\mathrm{B}^2-\mathrm{AC})^{1/2}} e^{[2\gamma(\mathrm{B}^2-\mathrm{AC})^{1/2}]}$$

(3) If $S_r = \dfrac{R}{(R^2-1)}$ then,

$$\phi = \arctan\left\{\frac{1}{\mathrm{C}}\left[\frac{\mathrm{B}+\mathrm{C}\tan\phi_0}{1-\gamma(\mathrm{B}+\mathrm{C}\tan\phi_0)} - \mathrm{B}\right]\right\}. \quad \text{(A7)}$$

APPENDIX 2

In most cases the best way to make the estimates of W_m is by using the Mohr circle construction (Means 1982, 1983, De Paor & Means 1984, Passchier 1988b, Wallis 1992a). The Mohr construction can also be used to derive the analytical solutions which are given in the main text. These equations have the advantage that they can be used without first studying the Mohr construction. The two main equations are derived below.

(i) Derivation of equation relating stretch along flow plane (A_1) to R_f and W_m.

From Fig. A1, the stretch along the flow plane, A_1, can be written as

$$A_1 = (T^2 - Q^2)^{1/2} + (R^2 - Q^2)^{1/2}. \quad \text{(B1)}$$

Because $S_1 = R_f^{1/2}$ and $S_2 = R_f^{-1/2}$

$$T = \tfrac{1}{2}(R_f^{1/2} + R_f^{-1/2}),$$
$$R = \tfrac{1}{2}(R_f^{1/2} - R_f^{-1/2}),$$
$$Q = W_m R$$

(Passchier 1988a,b). The above equations allow A_1 to be found once the mean vorticity number W_m and the X–Y strain ratio, R_f, are known. Substitution gives the rather cumbersome expression

$$A_1 = \tfrac{1}{2}(1 - W_m^2)^{1/2}\left[\left(R_f + R_f^{-1} + 2\frac{(1 + W_m^2)}{(1 - W_m^2)}\right) + (R_f + R_f^{-1} - 2)^{1/2}\right]. \tag{B2}$$

(ii) Derivation of equation relating W_m, β and R_f.

The three quantities W_m, β and R_f can be plotted on the Mohr circle in stretch space as shown in Fig. A1 (see also Passchier 1988b, Wallis 1992a). Wallis (1992a) shows that:

$$\tan\phi = \frac{R \sin 2\beta}{T - R\cos 2\beta},$$

therefore from Fig. A1

$$\frac{Q}{(T^2 - Q^2)^{1/2}} = \frac{R \sin 2\beta}{T - R\cos 2\beta}. \tag{B3}$$

After rewriting R, T and Q in terms of R_f, equation (B3) becomes

$$\frac{\tfrac{1}{2}W_m(R_f^{1/2} - R_f^{-1/2})}{\tfrac{1}{2}[(R_f^{1/2} + R_f^{-1/2})^2 - W_m^2(R_f^{1/2} - R_f^{-1/2})^2]^{1/2}} = \frac{\tfrac{1}{2}(R_f^{1/2} - R_f^{-1/2})\sin 2\beta}{\tfrac{1}{2}(R_f^{1/2} + R_f^{-1/2}) - \tfrac{1}{2}(R_f^{1/2} - R_f^{-1/2})\cos 2\beta}$$

and so

$$W_m[(R_f^{1/2} + R_f^{-1/2}) - \cos 2\beta(R_f^{1/2} - R_f^{-1/2})] = \sin 2\beta\,[(R_f^{1/2} + R_f^{-1/2})^2 - W_m^2(R_f^{1/2} - R_f^{-1/2})^2]^{1/2}.$$

After squaring both sides, the left-hand side (LHS) becomes:

$$\begin{aligned}\text{LHS} &= W_m^2[(R_f^{1/2} + R_f^{-1/2})^2 + \cos^2 2\beta(R_f^{1/2} - R_f^{-1/2})^2 \\ &\quad - 2\cos 2\beta(R_f^{1/2} - R_f^{-1/2})(R_f^{1/2} + R_f^{-1/2})] \\ &= W_m^2[R_f + R_f^{-1} + 2 + \cos^2 2\beta(R_f + R_f^{-1} - 2) \\ &\quad - 2\cos 2\beta(R_f + R_f^{-1})]\end{aligned}$$

and the right-hand side (RHS) becomes:

$$\text{RHS} = \sin^2 2\beta[R_f + R_f^{-1} + 2 - W_m^2(R_f + R_f^{-1} - 2)].$$

Multiplying both sides by R_f and collecting terms in R_f these become:

$$\begin{aligned}\text{LHS} &= R_f^2(W_m^2 + W_m^2\cos^2 2\beta - 2W_m^2\cos 2\beta) \\ &\quad + R_f(2W_m^2 - 2W_m^2\cos^2 2\beta) + W_m^2 \\ &\quad + W_m^2\cos^2 2\beta + 2W_m^2\cos 2\beta\end{aligned}$$

and

$$\begin{aligned}\text{RHS} &= R_f^2(\sin^2 2\beta - W_m^2\sin^2 2\beta) + R_f(2\sin^2 2\beta + 2W_m^2\sin^2 2\beta) \\ &\quad + \sin^2 2\beta - W_m^2\sin^2 2\beta\end{aligned}$$

Subtracting RHS from LHS gives

$$\begin{aligned}&R_f^2(2W_m^2 - 2W_m^2\cos 2\beta - \sin^2 2\beta) - 2R_f(\sin^2 2\beta) \\ &\quad + 2W_m^2 + 2W_m^2\cos 2\beta - \sin^2 2\beta = 0\end{aligned} \tag{B4}$$

which allows the strain ratio R_f to be calculated from known values of β and W_m using the standard solution to a quadratic equation.